

ELECTRONIC SUPPLEMENTARY INFORMATION

Vanadyl sulfates: molecular structure, magnetism and electrochemical activity

Anna Ignaszak^{a*}, Nigel Patterson,^a Mariusz Radtke,^a Mark R. J. Elsegood,^b Josef W. A. Frese,^b Joah L. Z. F. Lipman,^b Takehiko Yamato,^c Sergio Sanz,^d Euan Brechin,^d Timothy J. Prior^e and Carl Redshaw^{e*}

^a Department of Chemistry, University of New Brunswick, 30 Dineen Drive, Fredericton, NB, E3B 5A3, Canada.

^b Chemistry Department, Loughborough University, Loughborough, LE11 3TU, UK.

^c Department of Applied Chemistry, Faculty of Science and Engineering, Saga University, Honjo-machi, 840-8502, Saga-shi, Japan.

^d EaStCHEM School of Chemistry, University of Edinburgh, David Brewer Road, Edinburgh, EH9 3FJ, Scotland.

^e Chemistry, School of Mathematics & Physical Sciences, University of Hull, Cottingham Road, Hull, HU6 7RX, UK.

Table of Contents

I. Structural work

Figure S1. Alternative views of $1 \cdot \frac{1}{2}H_2O$.

Figure S2. Layer structure observed for $1 \cdot \frac{1}{2}H_2O$.

Figure S3. Alternative views of **2**.

Figure S4. Packing structure observed for **2**.

Figure S5. Alternative views of $3 \cdot MeCN$.

Figure S6. 2D sheet structure observed for **3**.

Figure S7. Alternative view of **4** with *tert*-butyl groups removed.

Figure S8. Mass spectrum of the precursor *p-tert*-butylsulfonylcalix[4]areneH₄.

Figure S9. Alternative views of **5**.

Figure S10. Alternative view of **6** and weakly-bound 3D network structure observed for **6**.

Crystallography experimental.

II. Electrochemistry

Experimental

Figure S11. DPV scans for various concentrations of compound **2** in 0.1M TEABF₄/ dry CH₃CN (absence of water, A); at the electrolyte : water = 10:1 v/v (B); and overlay of DPV scan for 0.75 mM in dry electrolyte (black) and in the presence of H₂O (blue); potentials quoted vs Ag/Ag⁺ (0.681 vs SHE).

Figure S12. CV scanning of compound **2** (0.75 mM) in 0.1M TEABF₄/ dry CH₃CN, vs Ag/Ag⁺ (0.681 vs SHE) in the absence (A) and presence of water (B) in the electrolyte : water = 10:1 v/v; potential scan rate 0.025 V/s.

Figure S13. CV recorded at various potential scan rates for compound **2** (0.75 mM) in 0.1M TEABF₄/ dry CH₃CN in the absence (A) and presence of water (B) in the electrolyte : water = 10:1 v/v; potential quoted vs Ag/Ag⁺ (0.681 vs SHE).

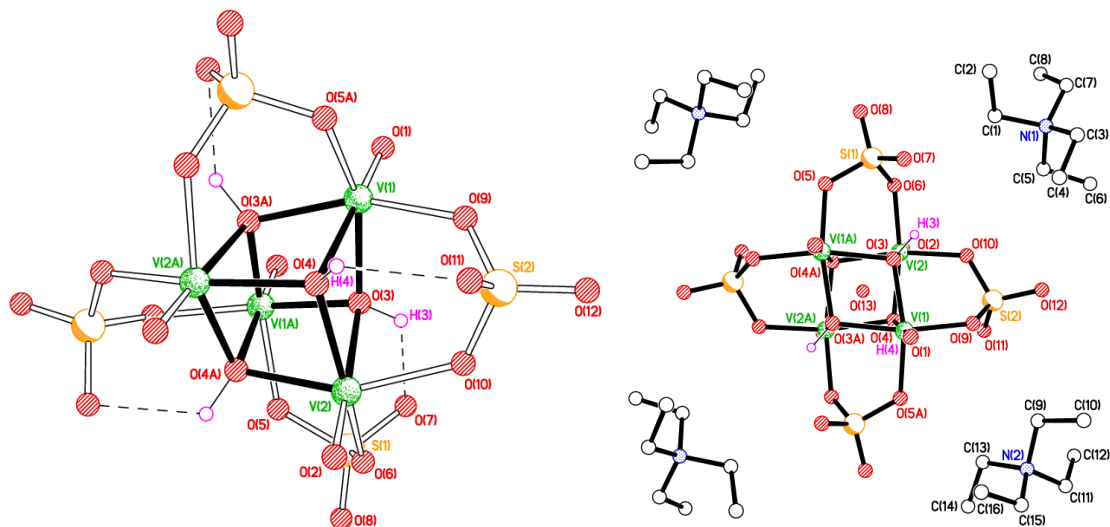
Figure S14. Bulk electrolysis (BE) carried out for 15 min at 1.4 V for various concentrations of compound **2** in the electrolyte : water = 10:1 v/v; potential quoted vs Ag/Ag⁺ (0.681 vs SHE). The slope of linear fit was used to calculate the rate of O₂ evolution in mmol O₂ per second and for TOF estimation (data presented in Table 1).

Figure S15. CV of 1 mM compound **5** in 0.1M TEABF₄/ dry CH₃CN, vs Ag/Ag⁺ (0.681 vs SHE) in the absence (black) and presence of water (blue) in the electrolyte : water = 10:1 v/v; potential scan rate 0.1 V/s.

Figure S16. Photos of compound **1** in 0.1M TEABF₄/ dry CH₃CN in the absence (A) and presence of water (B) in the electrolyte : water = 10:1 v/v, and after 100 CV scans were applied at the scan rate of 0.1 V/s to both solutions.

Figure S17. DPV (A) and CV (B) of compound **1** (1 mM) in 0.1M TEABF₄/ dry CH₃CN, vs Ag/Ag⁺ (0.681 vs SHE) in the absence (black) and presence of water (blue) in the electrolyte : water = 10:1 v/v; potential scan rate 0.1 V/s.

I. Structural work



Figures S1. Alternative views of $1 \cdot \frac{1}{2} \text{H}_2\text{O}$.

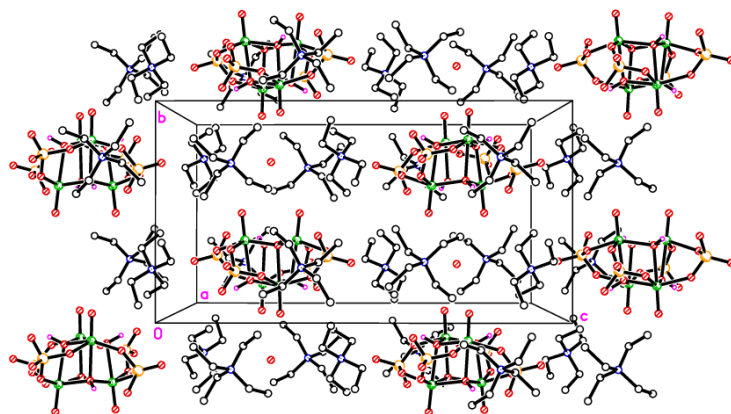


Figure S2. Layer structure observed for $1 \cdot \frac{1}{2} \text{H}_2\text{O}$.

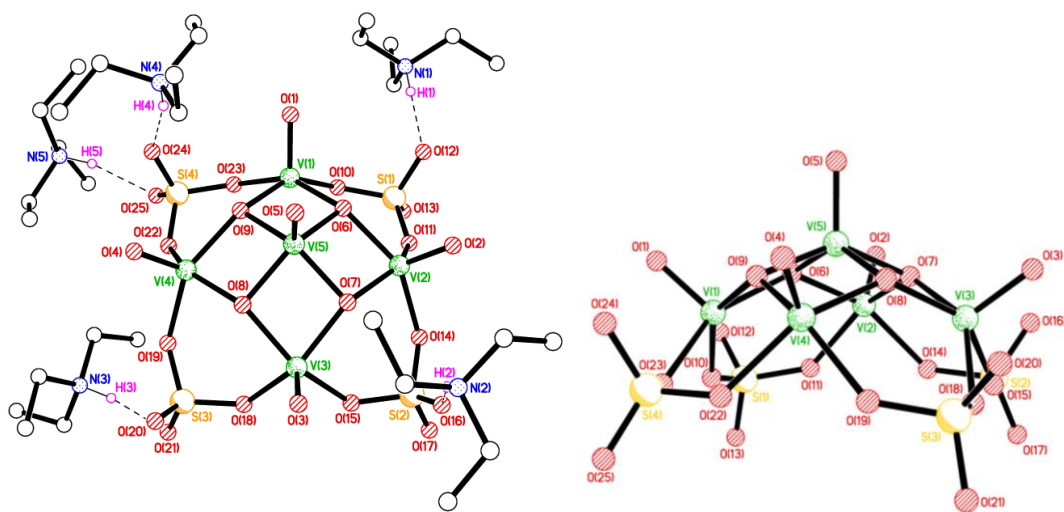


Figure S3. Alternative views of **2**.

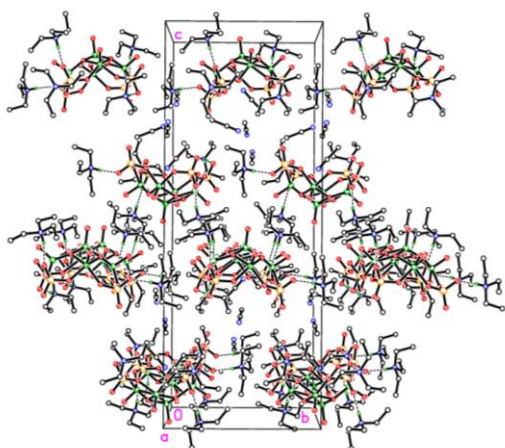


Figure S4. Packing structure observed for **2·4MeCN**.

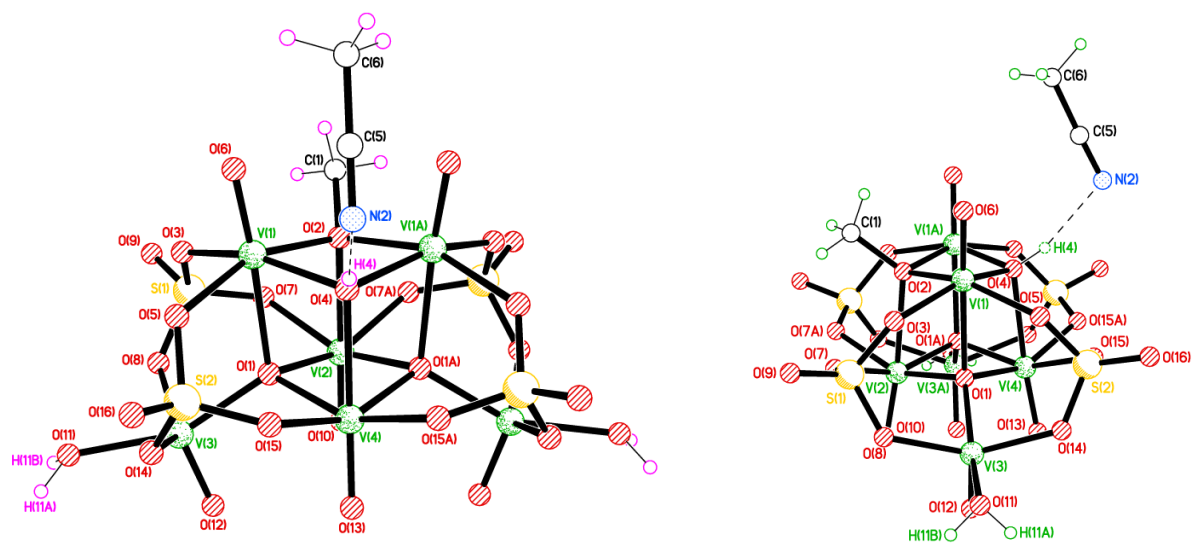


Figure S5. Alternative views of **3·MeCN**.

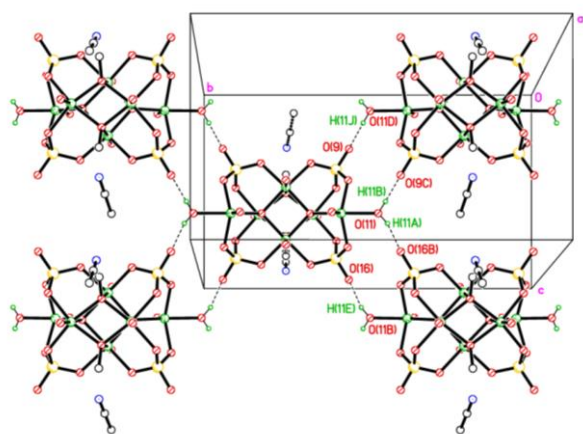


Figure S6. 2D sheet structure observed for **3·MeCN**.

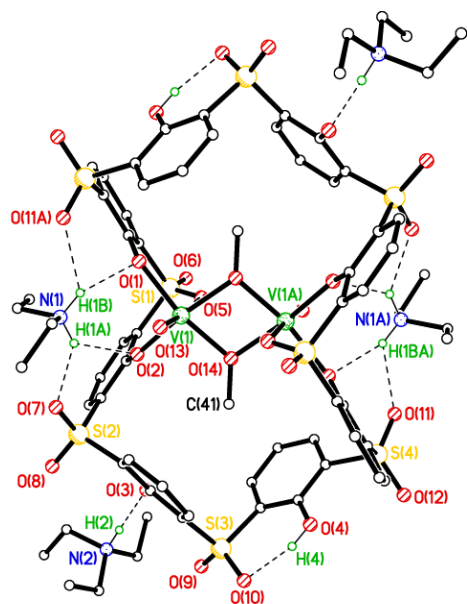


Figure S7. Alternative view of **4** with tBu groups removed.

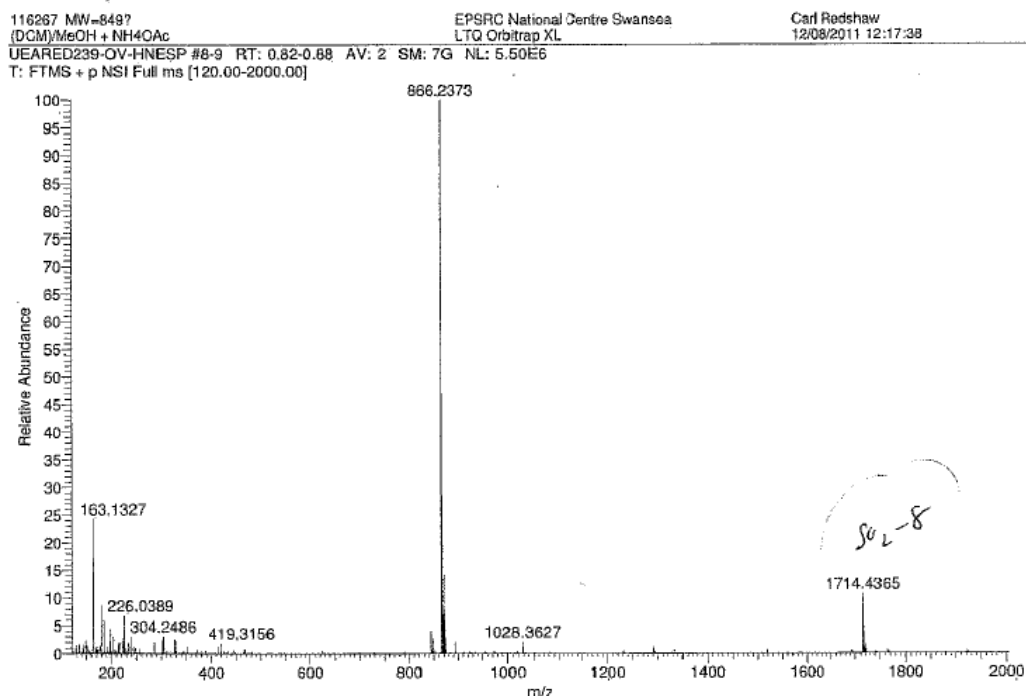


Figure S8. Mass spectrum of the precursor *p*-*tert*-butylsulfonylcalix[4]areneH₄.

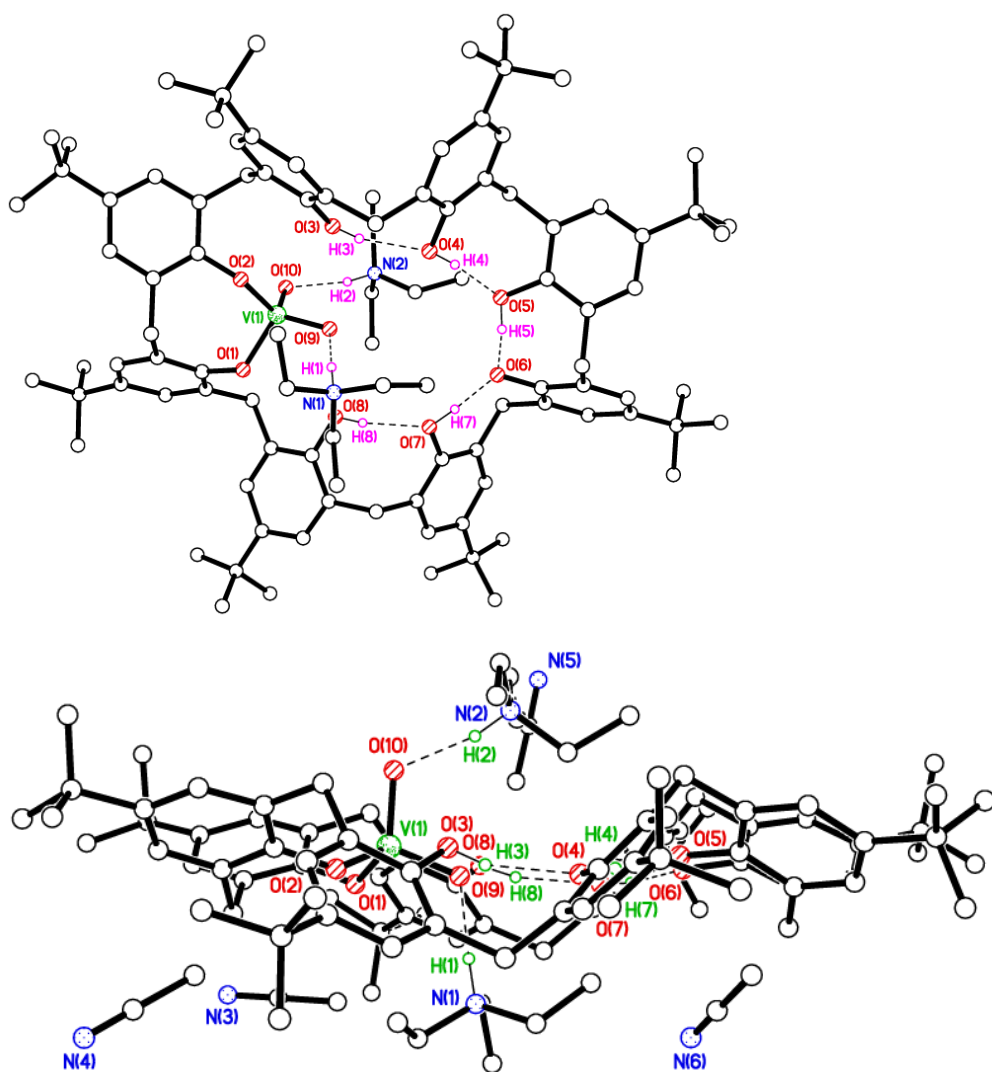


Figure S9. Alternative views of 5.

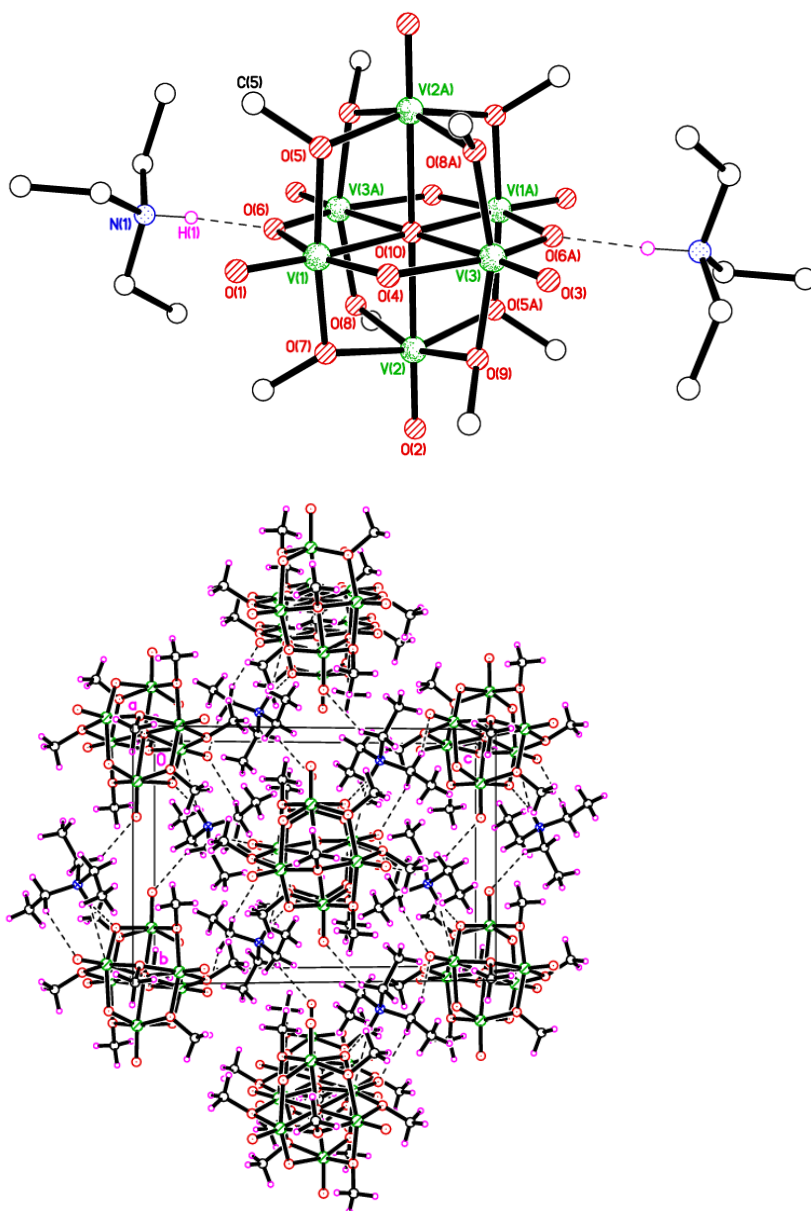


Figure S10. Alternative view of **6** and weakly-bound 3D network structure observed for **6**.

Crystallography experimental.

Crystal data are presented in the references in the main manuscript. Full details are given in the cif files deposited with the CCDC (see main manuscript for deposition numbers). Diffraction data were collected using CCD or image plate diffractometers using sealed tube or synchrotron X-ray sources. Data were corrected for Lp effects and absorption corrections were applied based on repeated

measurements. In $1\cdot\frac{1}{2}\text{H}_2\text{O}$ the water molecule was very diffuse or partially occupied and lies on a special position. It has reasonable H-bond distances to O(1) and O(2) and their symmetry equivalents. The molecule lies on a 2-fold axis and half is therefore unique. In $2\cdot 4\text{MeCN}$ in one of the $[\text{HNEt}_3]^+$ cations all three CH_2 groups were modelled as disordered over two sets of positions with major occupancy 64.8(5)%. The data was racemically twinned with major component 79.3(11)%. In $2\cdot\text{H}_2\text{O}$ there are two anions, ten cations and two water molecules in the asymmetric unit. The two anions are similar. The Et groups were modelled as split of two sets of positions in five out of the ten cations with some evidence of disorder in the others, though this was less severe, so not modelled. H atoms on water molecules could not be located in difference maps, but the oxygens were well behaved and have sensible H-bond distances to O(21), O(25), O(46) and each other. The diffraction data for $2\cdot 2.75\text{H}_2\text{O}$ were extremely weak. We therefore present only the unit cell and an approximate formula. This demonstrates the presence of the robust and clearly defined umbrella complex **2**, along with $[\text{NEt}_4]^+$ cations and some water molecules, the numbers of which could not be reliably ascertained due to the poor data quality and the complications of the imposed 4-fold crystallographic symmetry. For $3\cdot\text{MeCN}$ there is 50/50 methoxy/hydroxy disorder at O(2)/O(4). The OH atom was not refined, but its geometrically calculated position makes a good H-bond with the acetonitrile molecule. The data were twinned via a 180° rotation about reciprocal axis 1 0 0 with two domains and major component of 50.8(3)%. The molecule lies on a mirror plane. In **4** the phenol OH atom H(4) was found readily in difference maps. The $[\text{H}_2\text{NEt}_2]^+$ cation is required for charge balance and the possibility of this moiety being pentane or Et_2O is ruled out by the N atom U value becoming unreasonable if refined as C or O, respectively. Furthermore, the H-bonding is entirely reasonable. In $5\cdot 4\text{MeCN}$ methyl groups at C(18) and C(84) were modelled as two-fold disordered with major occupancy of 68.8(9) and 71.1(10)% respectively. OH coordinates and U_{iso} were refined while coordinates were refined for NH with U_{iso} tied to that of the N atom.

II. Electrochemistry

Experimental

Materials:

Silver nitrate (ACS reagent, $\geq 99.0\%$) and tetraethylammonium tetrafluoroborate, TEABF₄ (99%) were purchased from Sigma Aldrich, Canada. A dry acetonitrile was obtained from a home-installed solvent purification system (stainless steel construction equipped with column filled with activated molecular sieves type 5A, UNB, Fredericton, Canada).

Methods:

All electrochemical experiments were carried out on a CH Instruments electrochemical workstation model C440 coupled with the 400C series time-resolved electrochemical quartz crystal microbalance (EQCM). An electrochemical cell contained a platinum wire counter electrode, a non-aqueous Ag/Ag⁺ reference electrode (0.681 V vs. SHE, prepared by filling the electrode with solution of 0.01 M AgNO₃/0.1 M TEABF₄ in dry CH₃CN), and the glassy carbon resonator electrode with 0.1963 cm² area as a working electrode. All electrochemical measurements were carried out in 0.125 - 1 mM solution of the vanadium compounds dissolved in electrolyte. The CV scans were conducted in the potential range adjusted to the type of vanadium compounds in order to identify all redox peaks on voltammogram and with a potential scan rate varying from 0.025 to 3.0 V s⁻¹. The differential pulse voltammetry (DPV) technique was applied in order to improve peak separation and to eliminate the effect of charging current and was done in the potential range as for cyclic voltammetry, with the potential step increasing every 0.004 V and with a pulse width of 0.06 s, pulse period of 0.5 s, pulse amplitude of 0.05 V. The bulk electrolysis (BE) was carried out at the potential of water oxidation established based on CV and DPV scans for 15 min. The EQCM test was acquired before and after BE test in order to quantify the mass of produced monolayer of O₂. The stability of catalyst solution in dry electrolyte and in the presence of water (10:1 v/v) was carried out by recording 100 CV scans at 0.3 V s⁻¹. The

electrochemical stability was verified based on the comparison of peak position and peak current magnitude. For unstable compounds, the electrode cleaning step was introduced after each measurement by applying 100-300 CV scans between -2 and 2 V and with a scan rate of 0.3 V s^{-1} carried out in dry CH_3CN . In addition, the electrode was rinsed in dry ACN and electrolyte prior to next measurement. All experiments were taken in dry electrolyte 0.1 M TEABF_4 in CH_3CN and in electrolyte: $\text{H}_2\text{O} = 10:1 \text{ v/v}$, and the quantification of water oxidation product was carried out after subtraction of current/charge background in the absence of water (dry 0.1 M TEABF_4 in CH_3CN).

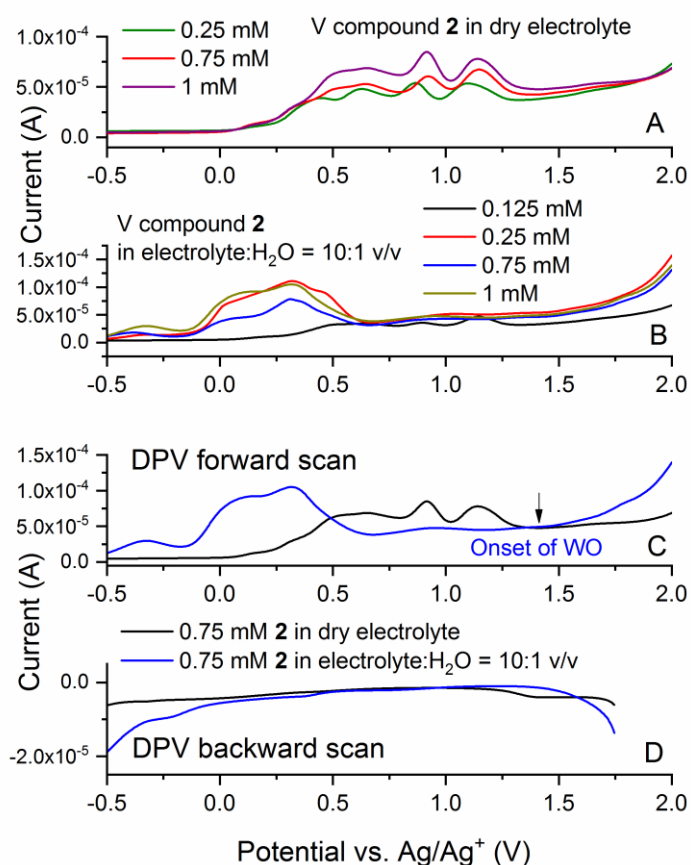


Figure S11. DPV scans for various concentrations of compound **2** in 0.1 M TEABF_4 / dry CH_3CN (absence of water, A); at the electrolyte : water = $10:1 \text{ v/v}$ (B); and overlay of DPV scan for 0.75 mM in dry electrolyte (black) and in the presence of H_2O (blue); potentials quoted vs Ag/Ag^+ (0.681 vs SHE).

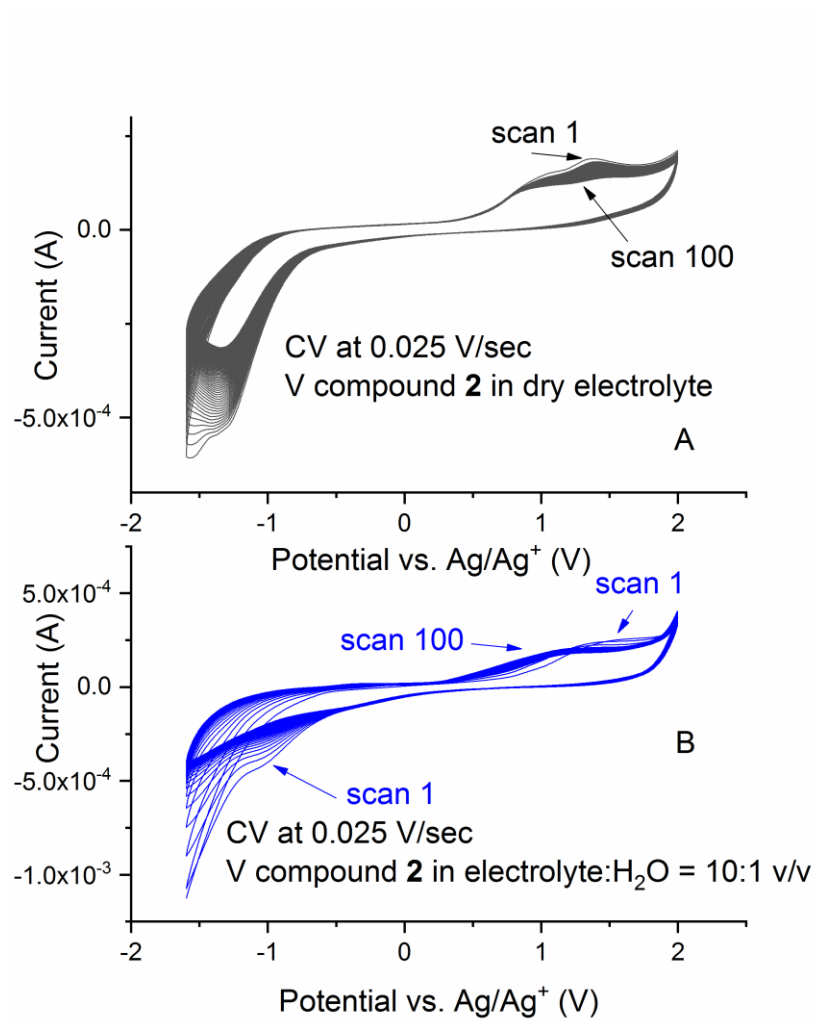


Figure S12. CV scanning of 0.75 mM **2** in 0.1M TEABF₄/ dry CH₃CN, vs Ag/Ag⁺ (0.681 vs SHE) in the absence (A) and presence of water (B) at the electrolyte : water = 10:1 v/v; potential scan rate 0.025 V/s.

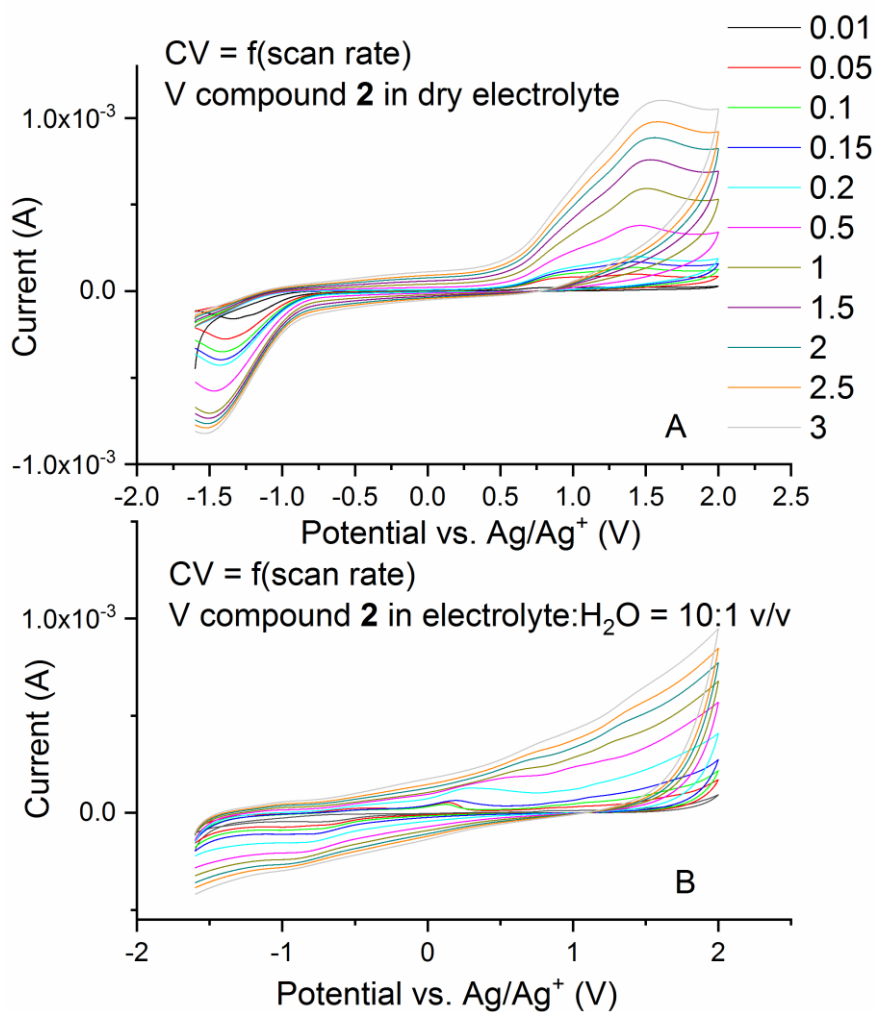


Figure S13. CV recorded at various potential scan rates for compound **2** (0.75 mM) in 0.1M TEABF₄/dry CH₃CN in the absence (A) and presence of water (B) in the electrolyte : water = 10:1 v/v; potential quoted vs Ag/Ag⁺ (0.681 vs SHE).

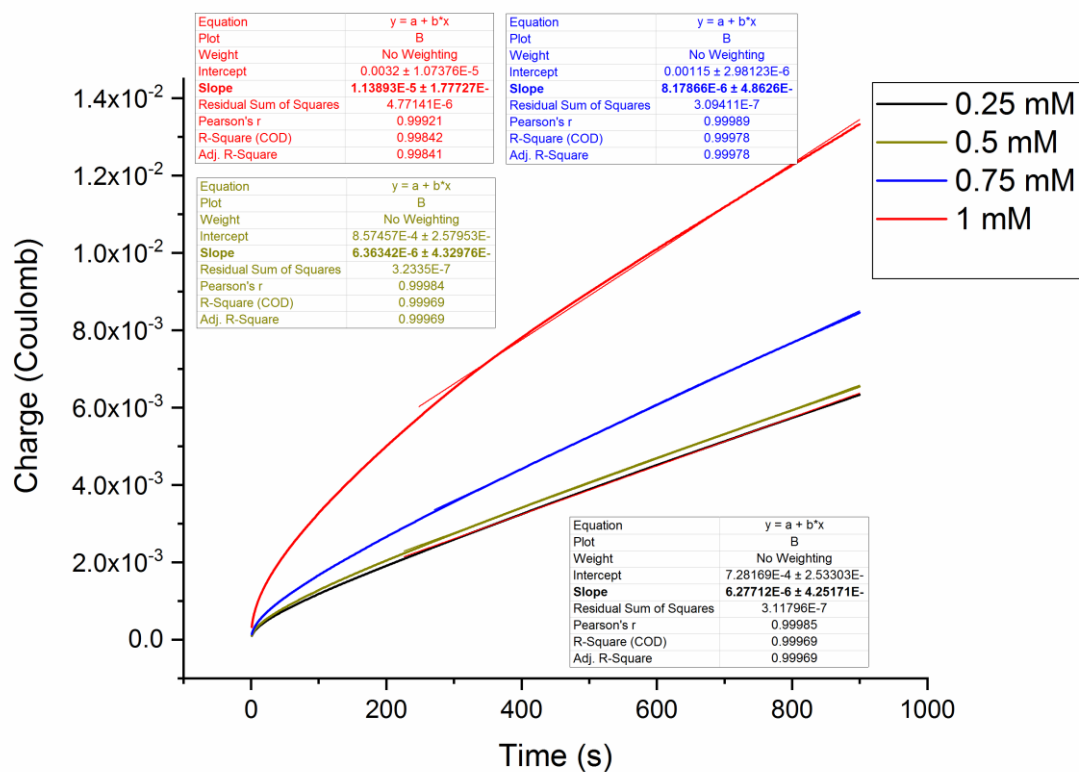


Figure S14. Bulk electrolysis (BE) carried out for 15 min at 1.4 V for various concentrations of compound **2** in the electrolyte : water = 10:1 v/v; potential quoted vs Ag/Ag⁺ (0.681 vs SHE). The slope of linear fit was used to calculate the rate of O₂ evolution in mmol O₂ per second and for TOF estimation (data presented in Table 1).

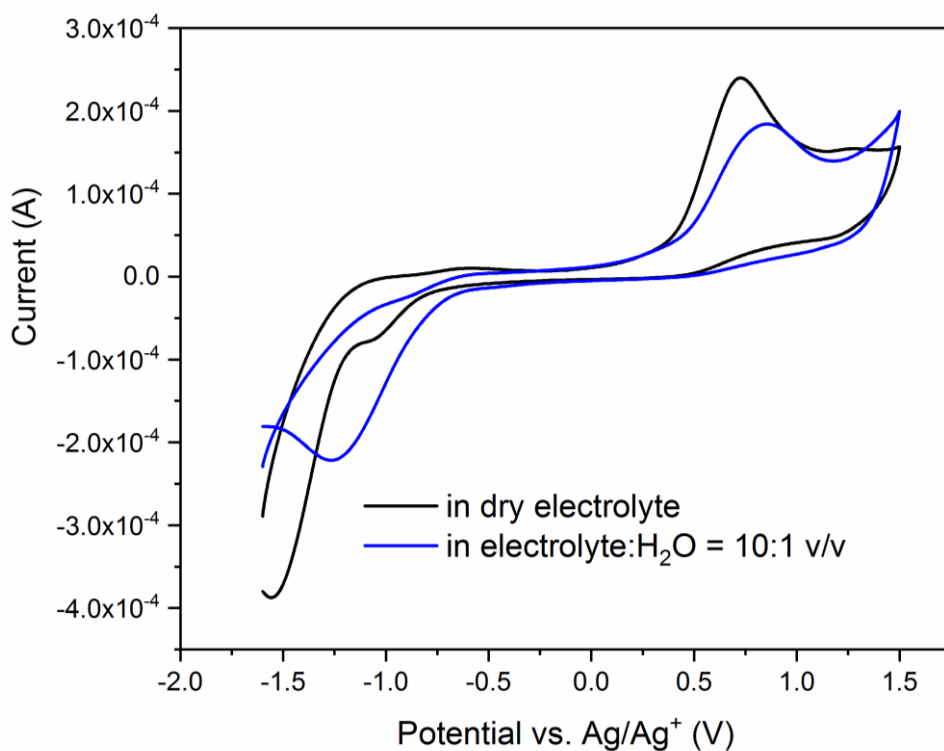


Figure S15. CV of 1 mM compound **5** in 0.1M TEABF₄/ dry CH₃CN, vs Ag/Ag⁺ (0.681 vs SHE) in the absence (black) and presence of water (blue) in the electrolyte : water = 10:1 v/v; potential scan rate 0.1 V/s.

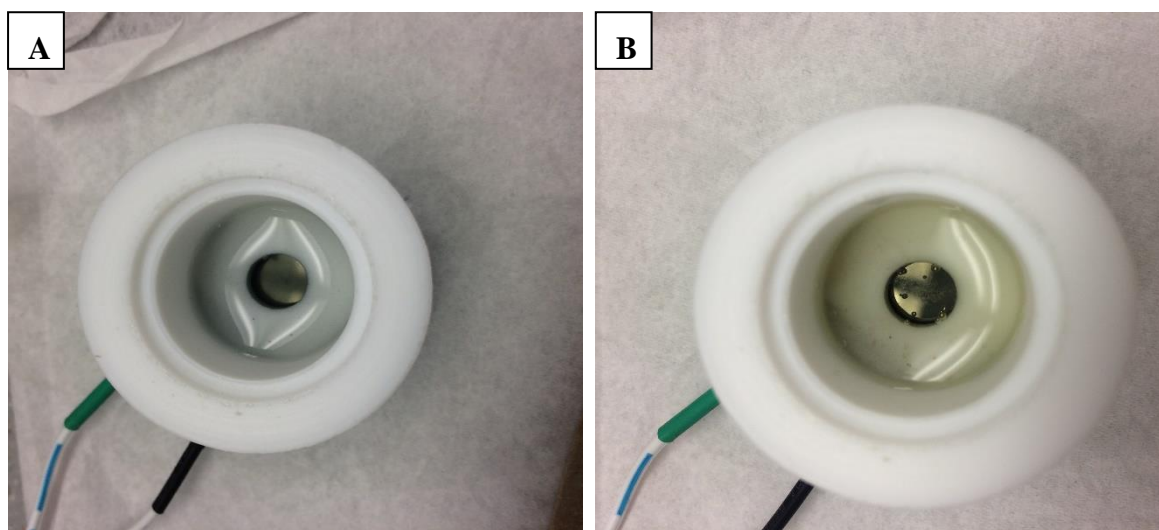


Figure S16. Photos of **1** solution in 0.1M TEABF₄/ dry CH₃CN in the absence (A) and presence of water (B) in the electrolyte : water = 10:1 v/v, and after 100 CV scans were applied at the scan rate of 0.1 V/s to both solutions.

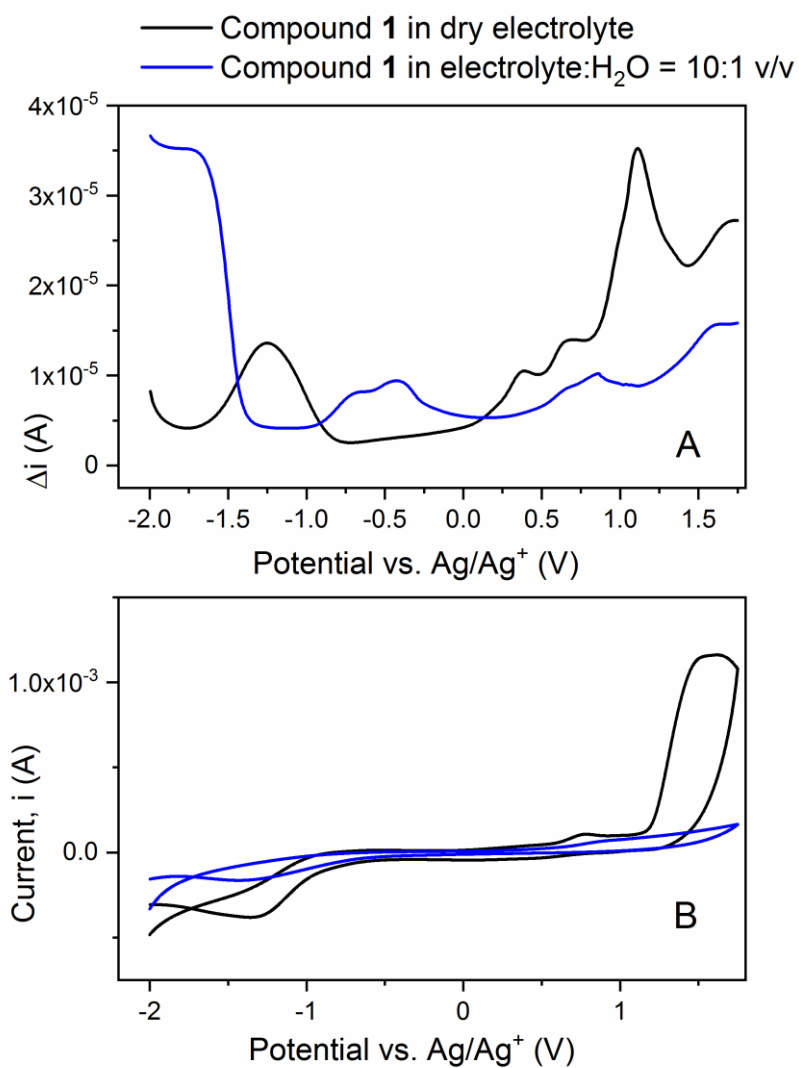


Figure S17. DPV (A) and CV (B) of compound **1** (1 mM) in 0.1M TEABF₄/ dry CH₃CN, vs Ag/Ag⁺ (0.681 vs SHE) in the absence (black) and presence of water (blue) in the electrolyte : water = 10:1 v/v; potential scan rate 0.1 V/s.